AGU PUBLICATIONS

JGR

Journal of Geophysical Research: Earth Surface

RESEARCH ARTICLE
10.1002/2014JF003180

Key Points:
- Fire changes soil thermal dynamics in tundra and boreal forest
- Changes in thermal conductivity determine the post fire soil thermal dynamics
- Tundra and boreal forest soils show different responses to fire

Supporting Information:
- Tables S1 and S2

Correspondence to:
Y. Jiang,
yjiang@mbl.edu

Citation:
Jiang, Y., A. V. Rocha, J. A. O'Donnell, J. A. Drysdale, E. B. Rastetter, G. R. Shaver, and Q. Zhuang (2015), Contrasting soil thermal responses to fire in Alaskan tundra and boreal forest, *J. Geophys. Res. Earth Surf.*, *120*, doi:10.1002/2014JF003180.

Received 15 APR 2014
Accepted 16 JAN 2015
Accepted article online 26 JAN 2015

Contrasting soil thermal responses to fire in Alaskan tundra and boreal forest

Yueyang Jiang[1], Adrian V. Rocha[2], Jonathan A. O'Donnell[3], Jessica A. Drysdale[1], Edward B. Rastetter[1], Gaius R. Shaver[1], and Qianlai Zhuang[4]

[1]The Ecosystems Center, Marine Biological Laboratory, Woods Hole, Massachusetts, USA, [2]Department of Biological Sciences and the Environmental Change Initiative, University of Notre Dame, Notre Dame, Indiana, USA, [3]Arctic Network, National Park Service, Fairbanks, Alaska, USA, [4]Department of Earth, Atmospheric, and Planetary Sciences, Purdue University, West Lafayette, Indiana, USA

Abstract Recent fire activity throughout Alaska has increased the need to understand postfire impacts on soils and permafrost vulnerability. Our study utilized data and modeling from a permafrost and ecosystem gradient to develop a mechanistic understanding of the short- and long-term impacts of tundra and boreal forest fires on soil thermal dynamics. Fires influenced a variety of factors that altered the surface energy budget, soil moisture, and the organic-layer thickness with the overall effect of increasing soil temperatures and thaw depth. The postfire thickness of the soil organic layer and its impact on soil thermal conductivity was the most important factor determining postfire soil temperatures and thaw depth. Boreal and tundra ecosystems underlain by permafrost experienced smaller postfire soil temperature increases than the nonpermafrost boreal forest from the direct and indirect effects of permafrost on drainage, soil moisture, and vegetation flammability. Permafrost decreased the loss of the insulating soil organic layer, decreased soil drying, increased surface water pooling, and created a significant heat sink to buffer postfire soil temperature and thaw depth changes. Ecosystem factors also played a role in determining postfire thaw depth with boreal forests taking several decades longer to recover their soil thermal properties than tundra. These factors resulted in tundra being less sensitive to postfire soil thermal changes than the nonpermafrost boreal forest. These results suggest that permafrost and soil organic carbon will be more vulnerable to fire as climate warms.

1. Introduction

Soils in boreal and arctic regions store large amounts of organic carbon in permafrost that are vulnerable to thaw and wildfire [*Schuur et al.*, 2008; *Balshi et al.*, 2009; *O'Donnell et al.*, 2011a]. Wildfires are increasing in these regions [*Kasischke and Turetsky*, 2006; *Hu et al.*, 2010; *Rocha et al.*, 2012] and can enhance permafrost thaw through processes that increase soil temperature and thaw depth over a variety of timescales [*Harden et al.*, 2006; *Kasischke et al.*, 2010]. Wildfires remove vegetation, decrease the thickness of the insulating soil organic layer, decrease albedo through surface charring, alter the surface energy balance, modify snow cover and depth, and change soil moisture [*Liu and Randerson*, 2008; *Rocha and Shaver*, 2011]. While each factor contributes to postfire soil warming, their relative influence on soil temperature remains poorly understood. However, determining the impact of each factor on soil warming is important and has implications for understanding the timescales in which fire alters the soil environment. For example, if albedo plays a large role in postfire soil warming, then postfire effects on soil temperature and thaw depth will be short lived and depend on the rate of canopy recovery. However, if decreases in organic-layer thickness play a large role in postfire soil warming, then postfire effects on soil temperature and thaw depth will be long lived and depend on both canopy recovery and the rate of soil organic matter accumulation [*Harden et al.*, 1997, 2006, 2012].

Fires can alter soil temperatures directly or indirectly through combustion of the organic layer. A reduction in the organic-layer thickness can directly impact soil temperature by increasing the efficiency in which heat is transferred through the soil, a process known as the thermal conductivity. Thermal conductivity is also influenced by other soil properties including soil texture and moisture. Interactions between the water-absorbing organic layer and soil moisture can indirectly impact soil temperature by increasing soil moisture and thermal conductivity. Generally, postfire impacts on organic-layer thickness and soil moisture increase soil temperature and deepen thaw depth, but the magnitude of this effect depends on whether soil thermal

conductivity responds linearly or nonlinearly to soil moisture and organic-layer thickness changes [*Yoshikawa et al.*, 2003; *Liljedahl et al.*, 2007].

Postfire changes to the surface energy balance can also affect soil temperature through changes in energy availability. Changes to the surface energy balance influence both soil and surface temperature in a variety of ways. Fires destroy the vegetation canopy, char the surface, and decrease surface albedo [*Chambers et al.*, 2005; *Rocha and Shaver*, 2009]. Surface albedo reductions can either increase or decrease available energy and surface temperature. The magnitude of these impacts depends on surface-atmosphere coupling and postfire energy partitioning toward latent and sensible heat fluxes [*Chambers et al.*, 2005]. The destruction of the vegetation canopy typically decreases surface roughness and surface-atmosphere coupling with the direct impact of decreasing available energy and increasing surface temperature. Postfire soil moisture changes also may indirectly influence soil and surface temperatures by altering energy partitioning. The destruction of the water-absorbing organic layer may increase surface moisture and cool the surface and increase available energy. Postfire interactions among energy availability, surface temperature, and soil temperatures are poorly understood but are thought to be largely dependent on postfire soil and ecosystem properties.

Postfire impacts on soil temperature and thaw depth also can vary across high-latitude ecoregions [*Rocha et al.*, 2012; *Shur and Jorgenson*, 2007] from differences in the presence or absence of permafrost. Arctic tundra is located in the continuous permafrost zone, and soil moisture is commonly at or near saturation [*Giblin et al.*, 1991]. In this region, high water tables atop the impervious permafrost may prevent large postfire changes to soil moisture or organic-layer thickness. In the boreal region of Alaska, the lack of permafrost may cause a greater reduction in the organic-layer thickness and a larger change in soil moisture, due to low water tables from deeper soils and the lack of an impervious permafrost layer [*Liu and Randerson*, 2008]. Permafrost and soil moisture interactions may play a large role in the recovery of postfire soil thermal conductivity because mosses and the organic layer recover more quickly (~10–20 years) in poorly drained soils than in well-drained soils [*Yi et al.*, 2009a; *Johnstone et al.*, 2010; *Jafarov et al.*, 2013]. Understanding the direct and indirect postfire impacts on soil temperature across permafrost and nonpermafrost Alaskan ecosystems has important implications for determining permafrost vulnerability to a future warmer world.

It is clear that postfire soil temperatures and thaw depth are influenced by the presence of permafrost, but the mechanisms behind these influences remain poorly understood, especially over long timescales. Here we use a soil thermal model [*Jiang et al.*, 2012] to examine both the short- and long-term postfire soil thermal dynamics in three contrasting regions including (1) an arctic tundra burn severity gradient located in the continuous permafrost zone, (2) a boreal forest fire chronosequence underlain by permafrost, and (3) a boreal forest fire chronosequence without permafrost. The goals of this study are to (1) validate a soil thermal model across different Alaskan ecosystems with field observations; (2) use both model parameters and field observations to determine the sensitivity of soil temperature to postfire surface temperature, organic layer, and soil moisture changes; and (3) use the model to determine postfire recovery time of soil temperature and thaw depth in tundra and boreal forests.

2. Methodology and Data Preparation

2.1. Field Observations

Soil temperature, soil moisture, and thaw depth measurements were collected from three study regions in Alaska (Figure 1). In arctic tundra on Alaska's North Slope, three sites were set up along a burn severity gradient (severe, moderate, and unburned) at the 2007 Anaktuvuk River fire scar to monitor surface energy exchange [*Rocha and Shaver*, 2011], soil temperature, and soil moisture. All three sites were underlain by permafrost and were characterized as poorly drained sites (Table 1). The entire soil organic layer was 3.8 and 5.8 cm thinner in the moderate and severe burn, respectively, than in the unburned site (control) [*Bret-Harte et al.*, 2013]. Soil temperature and soil moisture profiles were measured from 2008 to 2012. Soil temperature measurements at 2 and 6 cm depth were obtained using the averaged values from two soil thermocouples (TCAV-L; Campbell Scientific) [*Rocha and Shaver*, 2011]. Volumetric soil moisture (%) was measured at 2.5 cm depth using a CS616 soil moisture probe (Campbell Scientific). We will herein refer to the Anaktuvuk River sites as the tundra sites for clarity.

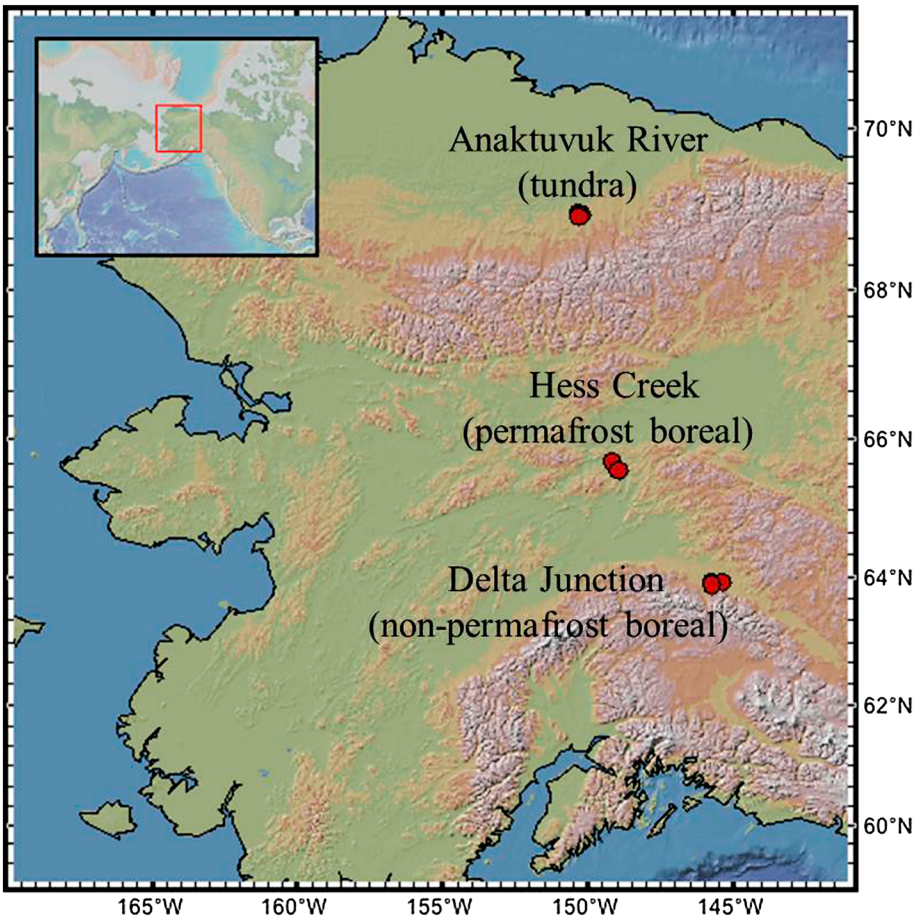

Figure 1. Map of Alaska with points showing the locations of the nine sites from three study regions: Anaktuvuk River (tundra), Hess Creek (permafrost boreal), and Delta Junction (nonpermafrost boreal).

The second set of soil temperature and moisture data were compiled from three upland sites near Hess Creek [*O'Donnell et al*., 2011a], located in Alaska's boreal region north of Fairbanks (Figure 1). Soil temperature and moisture were measured between 2007 and 2009 at an unburned mature black spruce (*Picea mariana*) stand and two stands that varied with time since fire (40 year burn and 4 year burn). Soil moisture was logged every 2 h using ECH_2O Smart Soil Moisture probes routed to a HOBO microstation (Onset, Inc., Bourne, MA, USA). Soil moisture probes were installed in distinct soil organic layers at each site, and also in the A mineral layer at the 4 year burn. Specifically, soil moisture was measured at depths 3, 7, and 22 cm for the unburned stand; at 18 cm for the 40 year burn; and at 6, 10, 18 cm for the 4 year burn. All three sites were located in north facing black spruce forests that were poorly drained and underlain by ice-rich permafrost. Relative to the control, the observed organic-layer thickness was ~10 cm thinner in the 4 year burn and 9 cm thinner in the 40 year burn. The maximum annual thaw depth was measured in late August at replicate locations within the control ($n = 32$), 4 year ($n = 21$), and 40 year ($n = 9$) stand ages. We will herein refer to the Hess Creek sites as the permafrost boreal forest for clarity.

The third data set was compiled from three boreal forest sites across a chronosequence near Delta Junction in interior Alaska measured between 2002 and 2004 (Figure 1) [*Liu et al*., 2005; *Liu and Randerson*, 2008]. A 1999 fire represented a 3 year old burn, a 1987 fire represented a 15 year old burn, and a ~1920 fire site represented a ~80 year old burn. Because data from an unburned site were unavailable at Delta Junction, a ~80 year stand was used as the unburned control. All three sites were well drained, underlain by coarse alluvial deposits, and generally lacked permafrost [*Welp et al*., 2007] though they were located in the discontinuous permafrost zone (50–90% of land area underlain by permafrost [*Harden et al*., 2006]). At all three sites, soil temperature was measured at 0, 2.5, 5, 10, and 20 cm using thermocouples [*Liu and Randerson*,

Journal of Geophysical Research: Earth Surface

10.1002/2014JF003180

Table 1. Description of Sites Used in This Study[a]

Region	Site	Location	Permafrost	Year Burned	Dominant Vegetation	Surface Roughness	Active Layer Depth (cm)	Organic Horizon Thickness (cm)	Moss Cover (%)	Volumetric Moisture Content[b] (%)	Period of Measurement	Reference
Tundra	Severe burn	68°59′4″N, 150°16′52″W	Continuous	2007	Graminoid tussock, 10% exposed mineral soil	0.02–0.03	56–69	11.6 ± 1.9	<5	51 ± 23 (2.5 cm)	2008–2012	*Rocha and Shaver* [2011] and *Bret-Harte et al.* [2013]
	Moderate burn	68°57′08″N, 150°12′43″W	Continuous	2007	Graminoid tussocks, non-*Sphagnum* mosses, and evergreen shrubs	0.02	52–67	15.4 ± 1.8	33	49 ± 17 (2.5 cm)		
	Unburned site	68°56′4″N, 150°16′22″W	Continuous	-	Graminoid tussocks, *Sphagnum* mosses, lichen, evergreen, and deciduous shrub	0.01–0.02	47–57	17.4 ± 2.1	40	56 ± 6 (2.5 cm)		
Permafrost boreal forest	4 year burn	65°34′7″N, 148°55′23″W	Discontinuous	2003	Standing dead black spruce, evergreen shrub, and moss (*Ceratodon purpureus*)	-	66 ± 12	14 ± 5	24	D (6 cm): 60 ± 13; M/H (10 cm): 63 ± 2; A (18 cm): 35 ± 1	2007–2009	*O'Donnell et al.* [2011a, 2011b]
	40 year burn	65°41′40″N, 149°7′54″W	Discontinuous	1967	Black spruce, Alaskan birch, evergreen shrub, and feather moss	-	54 ± 7	15 ± 4	35	M/H (18 cm): 65 ± 8		
	Control	65°34′3″N, 148°55′30″W	Discontinuous	1859	Black spruce, woody shrub, mosses, and lichen	-	45 ± 8	24 ± 5	95	L/D (3 cm): 7 ± 3 F (7 cm): 14 ± 4 M/H (22 cm): 36 ± 7		
Nonpermafrost boreal forest	3 year burn	63°55′N, 145°44′W	None	1999	Standing dead black spruce boles, grasses, evergreen shrubs, and deciduous shrubs	0.09	-	3.5	-	A (11 cm): 24 ± 3 gB (37 cm): 12 ± 1	2002–2004	*Manies et al.* [2004], *Chambers et al.* [2005], and *Liu and Randerson* [2008]
	15 year burn	63°55′N, 145°23′W	None	1987	Aspen and willow with patches of moss	-	-	5.7	-	A/B (11 cm): 18 ± 4 gB (37 cm): 22 ± 3		
	Control	63°53′N, 145°44′W	None	1920	Black spruce trees, feather moss, and lichen	0.70[c]	-	22	-	M (11 cm): 29 ± 4 gB (37 cm): 26 ± 4		

[a]The active layer depth (cm) is reported as the annual maximum thaw depth. Organic horizon thickness is reported as the mean thickness (cm) in the last year of measurement for each site.
[b]Volumetric water content is reported as the summer means. For the permafrost boreal forest, the letters represent soil horizons: L = live moss, D = dead moss, F = fibric, M = mesic, H = humic, A = A mineral horizon, and B = B mineral horizon. A lower case "g" indicates gravel was noted within the layer. The values in cm represent the depth below the ground surface where the soil moisture probe was installed. HC03 was the only site where soil moisture in mineral soil was monitored, mainly because the organic horizon was considerably thinner at this site.
[c]Surface roughness measured at an unburned spruce stand (63°48′N, 145°6′W) in Hajdukovich Creek in 1999 by *Chambers et al.* [2005].

2008]; soil moisture (volumetric soil water content) was measured at 2, 4, 11, and 37 cm by time domain reflectometry soil moisture sensors (CS615, Campbell Scientific, Inc.), as described in *Welp et al*. [2007]. The observed organic-layer thickness was 18.5 cm thinner in the 3 year and 16.3 cm thinner in the 15 year stand relative to the control (Table 1). We will herein refer to the Delta Junction sites as the permafrost boreal forest for clarity.

2.2. Model Simulations

We employed a soil thermal model [*Jiang et al*., 2012] to estimate the postfire changes in soil thermal conductivity and soil temperature at the tundra, permafrost, and nonpermafrost boreal forest. The model fully couples water flow and heat transport and is able to provide numerically stable, energy- and mass-conservative solutions [*Hansson et al*., 2004] and has been previously employed in boreal and tundra systems to simulate soil temperature gradients [*Jiang et al*., 2012]. Briefly, soil temperature was simulated numerically by solving a modified Richard equation [*Hansson et al*., 2004; *Saito et al*., 2006]. The governing equation for water flow is as follows [e.g., *Fayer*, 2000; *Noborio et al*., 1996]:

$$\frac{\partial\theta_u(h)}{\partial t}+\frac{\rho_i}{\rho_w}\frac{\partial\theta_i(T)}{\partial t} = \frac{\partial}{\partial z}\left[K_{Lh}(h)\frac{\partial h}{\partial z}+K_{Lh}(h)+K_{LT}(h)\frac{\partial T}{\partial z}+K_{vh}(\theta)\frac{\partial h}{\partial z}+K_{vT}(\theta)\frac{\partial T}{\partial z}\right] \tag{1}$$

where θ is the volumetric liquid water content (%), θ_u is the volumetric unfrozen water content (%), θ_i is the volumetric ice content (%); h is the pressure head (m), t is time (units), z is depth (m); T is the absolute temperature (K); ρ_i is the density of ice (931 kg m^{-3}) and ρ_w is the density of liquid water (1000 kg m^{-3}); K_{Lh} (m s^{-1}) and K_{LT} (m^2 K^{-1} s^{-1}) are the isothermal and thermal hydraulic conductivities for liquid-phase fluxes due to gradients in h and T, respectively; K_{vh}(m s^{-1}) and K_{vT}(m^2 K^{-1} s^{-1}) are the isothermal and thermal vapor hydraulic conductivities, both are functions of water content and temperature. The equations to calculate K_{vh} and K_{vT} are derived from *Saito et al*. [2006] (supporting information).

The governing function for heat transport is as follows:

$$\frac{\partial C_pT}{\partial t}-L_f\rho_i\frac{\partial\theta_i}{\partial t}+L_0(T)\frac{\partial\theta_v(T)}{\partial t} = \frac{\partial}{\partial z}\left[\lambda\frac{\partial T}{\partial z}\right]-C_w\frac{\partial q_lT}{\partial z}-C_v\frac{\partial q_vT}{\partial z}-L_0(T)\frac{\partial q_v}{\partial z} \tag{2}$$

where C_p (J m^{-3} K^{-1}) is the volumetric heat capacity of the soil and C_w (4.18×10^6 J m^{-3} K^{-1}) and C_v (1.2×10^3 J m^{-3} K^{-1}) are the volumetric heat capacities of the liquid and vapor phases, respectively; L_0 is the volumetric latent heat of vaporization of liquid water (J m^{-3}), and L_f is the latent heat of freezing (3.34×10^5 J kg^{-1}); λ is the apparent thermal conductivity of soil (J m^{-1} s^{-1} K^{-1}), which is a function of the ice (θ_i) and water (θ) contents indirectly related to soil temperature and freezing conditions (equation (3), where C$_i$ ($i=1,\ldots,5$), F_1, and F_2 are parameters); q_L and q_v are the flux densities of liquid water and water vapor (m s^{-1}), respectively; q_L and q_v are both functions of water content and temperature as calculated in *Fayer* [2000].

$$\lambda = C_1+C_2(\theta+F\theta_i) - (C_1-C_4)\exp\left\{-[C_3(\theta+F\theta_i)]^{C_5}\right\};\ \text{and}\ \ F=1+F_1\theta_i^{F_2} \tag{3}$$

We solved equations (1) and (2) numerically using a finite difference method for both spatial and temporal discretization. Measured daily ground surface temperatures were used as the model driver and the upper temperature boundary condition, while the measured soil moisture by the lowermost sensor as the upper boundary for the soil water cycle. Initial conditions for model runs were established through linear interpolation for the observed soil temperature profile.

In the model, the top 3.5 m of the soil profile was discretized into six layers (moss, fibrous, amorphous, and A/B/C mineral layers). The thickness of each layer was determined separately for each study site, based on field measurements [*Hinkel and Nelson*, 2003; *Bret-Harte et al*., 2013; *O'Donnell et al*., 2011a, 2011b; *Manies et al*., 2004]. The soil physical properties (e.g., volume fraction of solid) were implicitly accounted for in the parameterization for calculating thermal conductivity in each soil layer. To take into account the soil moisture

data, in the model simulations we linearly interpolated the measured soil moisture through the vertical soil profile for the upper layers in which measured moisture was available. Because soil moisture measurements were only available at 2.5 cm depth for the three tundra sites, we added measured soil moisture (at 9, 12, 38, 39, and 68 cm) from a nearby unburned Toolik Lake site (68°37′22.9″N, 149°36′35.4″W, http://soils.usda.gov/survey/smst/alaska/Toolik/ [*Hinkel and Nelson*, 2003]) to distribute the moisture through the vertical soil profile during the observation period.

Parameters used for all simulations at all sites were presented in Table S1 in the supporting information. For each of the six layers at each site, we calibrated the seven parameters (C_i ($i = 1,\ldots, 5$), F_1, and F_2) governing the thawed and frozen thermal conductivity in equation (3), to fit the modeled soil temperatures to in situ measurements. We did not recalibrate the parameters for calculating hydraulic conductivity but kept using the values for the tundra (Toolik Lake), permafrost boreal forest (Hess Creek), and nonpermafrost boreal forest (Bonanza Creek) sites studied in *Jiang et al*. [2012] (Table S2). The reasons were the following: (1) we prescribed soil moisture based on measurements for each depth in the layers where measurements were available. For the tundra and permafrost boreal forest sites, these measurements were the same data used to constrain the calibration of the hydraulic parameters in *Jiang et al*. [2012]. (2) For deep layers where moisture measurements were not available, we assumed that the corresponding tundra, permafrost boreal forest, and nonpermafrost boreal forest sites studied in *Jiang et al*. [2012] were representative in terms of soil type and porosity. This assumption would not significantly influence the results and conclusions of our study. (3) Calibrating hydraulic parameters to fit the soil temperature may cause overparameterization of the water cycle.

In the fitting for thermal conductivity, the fire-caused change in water cycle was taken into account through the prescribed soil moisture in the upper soil layers based on measurements. In particular, we prescribed the soil moisture at all depths within the uppermost 68 cm soil at the three tundra sites based on in situ measurements, while soil moisture below 68 cm was estimated according to model water balance equation with measured soil moisture at 68 cm as upper boundary condition. Similarly, we prescribed the soil moisture of all depths in top 18, 18, and 22 cm soil of the 4 year, 40 year and unburned Hess Creek stand, respectively. For all three Delta Junction stands, we prescribed the soil moisture of the top 37 cm and simulated the soil moisture below 37 cm by solving the water balance equation. For all simulations, we assumed no water flux at lower boundary. Soil temperature was calculated by solving the heat transfer equation with measured surface temperature or the uppermost sensor (if no surface temperature was measured) as upper boundary condition. We set the lower boundary condition as a heat flux of $\lambda(\theta)\frac{\partial T}{\partial z}$.

For layers with measurement, we recalibrated the model parameters; while for layers with no measurement, we kept using the default parameter values. In the calibration, we first conducted 10,000 sets of ensemble simulations, each with a unique combination of parameter values produced from a Latin Hypercube sample algorithm [*Iman and Helton*, 1988]. In the sampling process, each parameter was sampled uniformly across its range (±90% of the default value) and was assumed independent with each of the other parameters. We calculated the root-mean-square error (RMSE) between measured and modeled soil temperatures in each of the 10, 000 Monte Carlo simulations. Then we selected the 500 simulations with the lowest RMSEs among the ensemble simulations and calculated the covariance matrix among all calibrated parameters. Because no significant covariance was found among any pairs of parameters, no significant overparameterization existed. Eventually, the "optimal" parameters were determined by the set of parameters that minimized the RMSE. Our calibration scheme cannot guarantee to find the best set of parameters that completely avoided the possible overfitting issue, but it should be able to find a set close to the best. Moreover, because our study focused on the relative comparisons with the same methodologies, the overfitting issue should not significantly impact our results.

Using the optimized parameters, we first conducted simulations to estimate the soil thermal states at each study site, driven by the measured surface temperature. For the tundra sites, winter gaps in data (i.e., surface temperature and soil moisture) were filled using measurements from the unburned Toolik Lake site mentioned above. We then conducted sensitivity analyses to investigate the relative impact of postfire surface warming, reduction in organic-layer thickness, and moisture change on soil temperature. We focused our analyses on near-surface soil layers (top 20 cm), which contained most of the organic layer across all three control sites that we studied (Table 1). In particular, we assessed the responses of the mean thermal

conductivity of the top 20 cm (K_{20cm}) and soil temperature at 20 cm (T_{20cm}) to a set of manipulated perturbations of ground surface temperature, organic-layer thickness, and soil moisture. For the sensitivity analyses, changes in ground surface temperature, organic-layer thickness, and soil moisture based on observed variations from the study sites were prescribed to the model runs (Table 1). For the tundra sites, we imposed increases of summer daily surface temperature ranging from 0 to 1.1°C in 0.1°C intervals, organic-layer thickness ranging from 9 to 20 cm in 1 cm intervals, and soil moisture from 30% to 50% with 1% intervals. These ranges were determined by the maximum and minimum values from field measurements [*Rocha and Shaver*, 2011]. Similarly, based on measurements at the permafrost boreal forest and using the same increments used for the tundra burn, surface temperature was increased by 0 to 2°C, the remaining organic-layer thickness ranged from 13 to 25 cm, and the soil moisture ranged from 29% to 65%. At the nonpermafrost boreal forest, surface warming increased 0 to 7°C, the organic-layer thickness ranged from 4 to 22 cm, and the soil moisture ranged from 33% to 14% after fire. The measured summer surface temperature, organic-layer thickness, and soil moisture at the control sites were used as the base values upon which the corresponding perturbations were prescribed.

To predict the future thaw depth in each study site throughout the next 100 years after observations, we conducted simulations under four HadCM3 climate change scenarios (A1FI, A2, B1, and B2 [*Intergovernmental Panel on Climate Change*, 2007]). The soil moisture was calculated by solving the water balance equation with upper boundary condition forced by the global climate model-derived precipitation and potential evapotranspiration. No lateral water fluxes were included and zero water flux was assumed at the lower boundary. The postfire recovery rate of the moss layer was based on an empirical function [*Yi et al*., 2009a, 2010; *Yuan et al*., 2012; *Jafarov et al*., 2013]. In particular, the moss layer thickness (cm) was calculated as

$$d_{\mathrm{moss}} = d_{\mathrm{moss,max}} \frac{y_{\mathrm{sf}}}{y_{\mathrm{sf}} + y_{\mathrm{half}}}$$

where $d_{\mathrm{moss,max}}$ was the maximum thickness of moss (cm), y_{sf} was number of years since fire, and y_{half} was number of years needed for moss to reach half of the maximum. In our study, $d_{\mathrm{moss,max}}$ was determined for each study region based on the measurements at the control site; y_{half} was assigned 5 for the nonpermafrost boreal forest based on *Yi et al*. [2009b], and 3 for tundra and permafrost boreal forest based on the assumption that moss layer recovery in the poorly drained soils (~10–20 years) is faster than in well-drained soil [*Yi et al*., 2009a; *Johnstone et al*., 2010; *Jafarov et al*., 2013]. For the fibrous and amorphous layers, we used a similar function as in *Kasischke and Johnstone* [2005]

$$d = a - \frac{200}{b + y_{\mathrm{sf}}}$$

where d is the thickness of fibrous or amorphous layer, parameters a and b are fitted separately in the permafrost and nonpermafrost boreal forest, and the value b for tundra was assumed to be similar to the permafrost boreal forest. During the long-term simulations, the parameters used to calculate hydraulic conductivity were kept constant. Therefore, the effect of moss recovery on the hydraulic conductivity was through the changes in soil temperature and soil moisture.

2.3. Quantifying Postfire Impacts

Postfire changes to soil temperature, thaw depth, and thermal conductivity were determined as differences (Δ) between the burned and unburned site for each location [*Rocha and Shaver*, 2011]. This was done to isolate the postfire impact on soil thermal properties, directly compare the burned sites to an unburned control, and minimize differences in climate among the boreal and tundra sites. A positive Δ indicated that fire increased a particular variable, whereas a negative Δ indicated that the fire decreased a particular variable. A zero Δ indicates postfire recovery of the particular variable.

3. Results

3.1. Comparison Between Modeled and Measured Soil Temperatures

Modeled soil temperatures (Figure 2) agreed well with the measurements at each site, with fairly small RMSEs (~1 to 3°C) that increased slightly with soil depth (Table 2). The model overestimated soil temperatures when soils were close to freezing (e.g., by about 1–3°C at the 5 cm soil, Figure 2) at the three tundra sites. At the burned permafrost boreal forest, especially at the more recent 4 year burn, the model predicted slightly

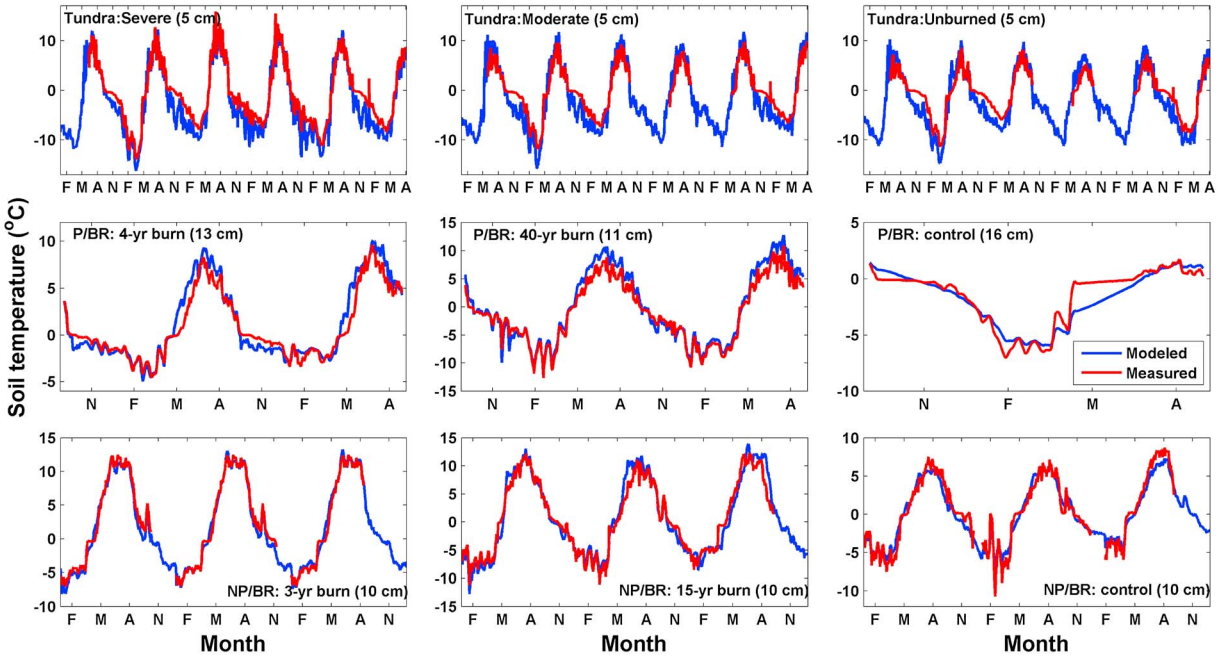

Figure 2. Comparison between the simulated and observed soil temperature at all study sites. F = February, M = May, A = August, and N = November. S = Severe, M = Moderate, and U = Unburned; "P" is permafrost, "NP" is nonpermafrost, and "BR" is boreal forest.

higher soil temperatures during spring and a faster thaw than observations. At the control stand in permafrost boreal forest, the model underestimated soil temperatures during spring thaw when observations indicated that soil temperatures hovered around 0°C for about 2 months. The model performed well in simulating summer soil temperatures across all depths and sites with no systemic bias (Figure 2).

3.2. Postfire Changes in Surface and Soil Temperatures

3.2.1. Comparison of Measured Postfire Surface Temperature Among Different Ecosystems

Generally, postfire surface warming was greater in the boreal forest than in tundra (Figure 3b). In the severely burned tundra surface temperatures were ~1.0°C higher the year after the fire and decreased over time with a cooler surface than the control in the last 3–5 years. Measured surface temperatures in the moderate tundra burn were slightly lower than the control with a slight cooling trend throughout the five postfire years.

Table 2. The Root-Mean-Square Error (RMSE, °C) Values From the Linear Regression Between Modeled and Measured Soil Temperatures (°C) Across the Tundra (Anaktuvuk River Sites), the Permafrost Boreal Forest (Hess Creek), and the Nonpermafrost Boreal Forest (Delta Junction) Stands

Depth	ARF-S	ARF-M	ARF-U	HC03	HC67	HCCN	DJ99	DJ87	DJ-C
3 cm							0.72	1.11	0.81
5 cm	1.38	1.50	1.54			2.77	0.80	1.29	0.85
6 cm					1.48				
8 cm				0.79					
10 cm	1.83	2.25	2.14				0.79	1.41	0.81
11 cm					2.26				
13 cm				1.23					
16 cm						1.67			
20 cm	2.49	2.77	2.23		1.90		1.82	1.91	1.64
30 cm	2.38	3.01	1.92						
40 cm	2.74	2.91	2.64						
51 cm						2.42			
74 cm					2.71				
81 cm				0.49					
200 cm						1.75			

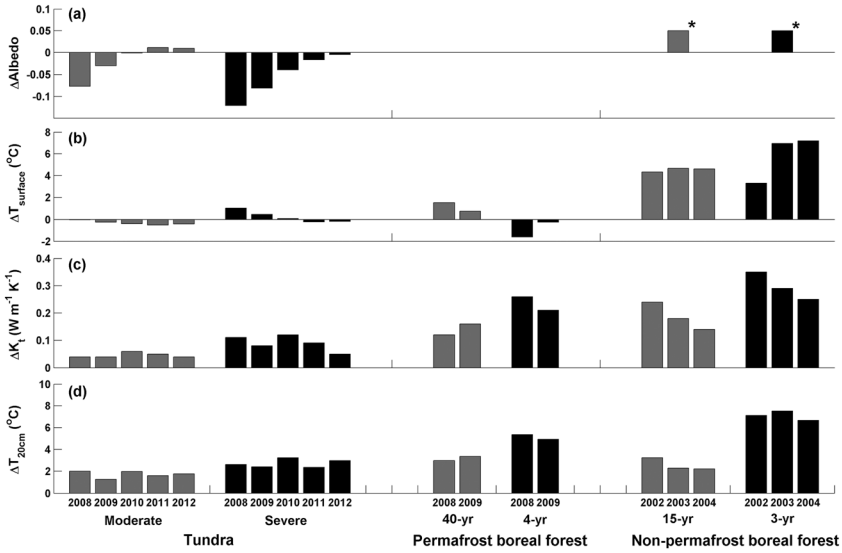

Figure 3. Differences between burned and unburned sites in (a) summer mean albedo, (b) summer surface temperature, (c) summer thermal conductivity of the top 20 cm soil, and (d) summer soil temperature at 20 cm, from 2008 to 2012 at the tundra fire scar, from 2008 to 2009 at the permafrost boreal forest, and from 2002 to 2004 at the nonpermafrost boreal forest. Each bar represents a specific year. It should be noted that the albedo for the 15 year stand in nonpermafrost boreal forest is measured in 1999 by *Chambers and Chapin* [2002], and for the 3 year stand is the 3 year mean value.

In contrast, at the permafrost boreal forest, the measured mean summer (June through August) surface temperatures were 0.8–1.5°C higher at the 40 year old stand, and 0.3–1.6°C lower at the 4 year stand (Figure 3b), relative to the control. At the nonpermafrost boreal forest, observed surface temperatures were 4.5°C warmer at the 15 year stand and 5.8°C warmer at the 3 year stand, relative to the control (Figure 3b).

3.2.2. Thermal Conductivity

Postfire soil thermal conductivity within the upper 20 cm (K_{20cm}) increased in burned areas across all three studied regions. At the tundra sites, modeled summer (June through August) K_{20cm} was 0.04–0.06 W m^{-1} K^{-1} higher at the moderately burn site, and 0.05–0.12 W m^{-1} K^{-1} higher at the severely burned site, relative to the control (0.11–0.14 W m^{-1} K^{-1}). At the permafrost boreal forest, K_{20cm} was 0.12–0.16 W m^{-1} K^{-1} higher in the 40 year stand, and 0.21–0.26 W m^{-1} K^{-1} higher in the 4 year stand, relative to the control (~0.12 W m^{-1} K^{-1}). At the nonpermafrost boreal forest, K_{20cm} was 0.14–0.24 W m^{-1} K^{-1} higher at the 15 year stand, and 0.25–0.35 W m^{-1} K^{-1} higher at the 3 year stand, relative to the control (0.19–0.22 W m^{-1} K^{-1}, Figure 3c). Generally, postfire increases in soil thermal conductivity were smaller in tundra than in the boreal forest (Figure 3c).

Modeled frozen thermal conductivity in winter was higher than the summer thawed thermal conductivity (Table 3). Summer and winter thermal conductivity differences were larger at the burned sites for both tundra and permafrost boreal forest, mainly because of the higher ice content at the burned sites. Burned permafrost boreal forest had slightly higher summer and winter thermal conductivity differences than burned tundra.

Table 3. The Simulated Summer and Winter Soil Thermal Conductivities and the Difference (Δ) Between Winter Frozen Conductivity and Summer Thawed Conductivity in Sites Underlying by Permafrost

Region	Site	Summer Thermal Conductivity (W m^{-1} K^{-1})	Winter Thermal Conductivity (W m^{-1} K^{-1})	Δ
Tundra	Severe	0.22	0.53	0.31
	Moderate	0.18	0.47	0.29
	Control	0.13	0.38	0.25
Permafrost boreal forest	4 year	0.35	0.72	0.37
	40 year	0.32	0.89	0.57
	Control	0.12	0.35	0.23

3.2.3. Soil Temperature

Postfire summer soil temperatures were warmer at the burned sites, especially at the severe tundra burn immediately after fire, and at the young boreal forest stand (Figure 3d). In tundra, summer soil temperatures at 20 cm (T_{20cm}) were 1.3–2.0°C higher in the moderately

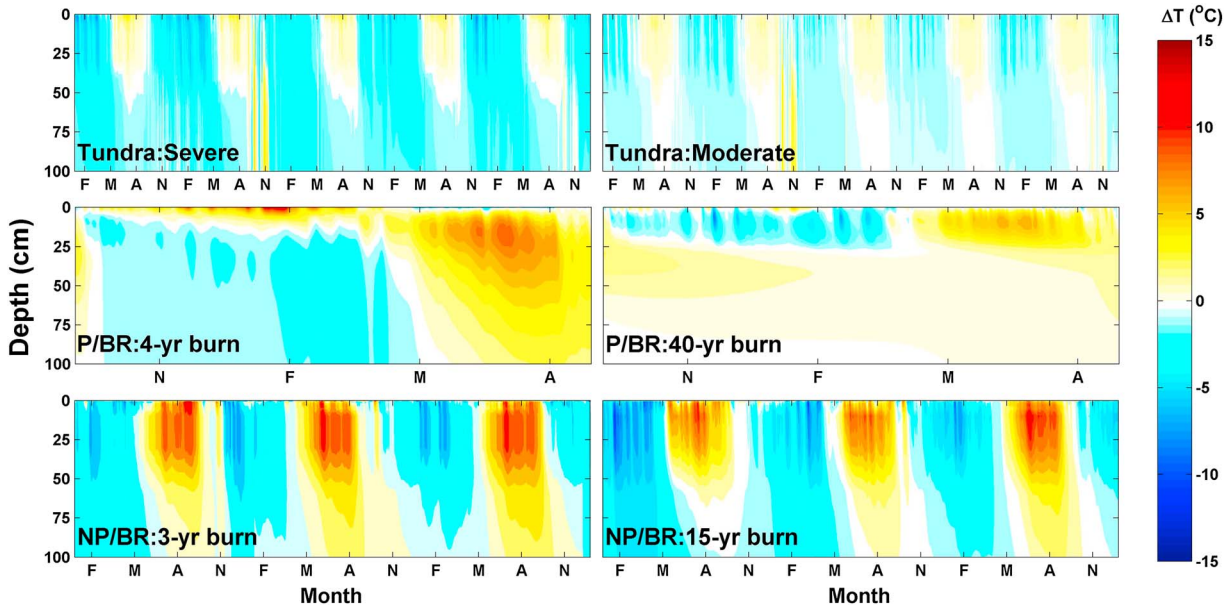

Figure 4. Difference in simulated soil temperatures between burned sites and the control for the top 20 cm of soil, at the severely and moderately burned sites in the tundra, the 4 year and 40 year stands at the permafrost (P) boreal forest (BR), and the 3 year and 15 year stands at the nonpermafrost (NP) boreal forest. F = February, M = May, A = August, and N = November.

burned site, and 2.4–3.2°C higher in the severely burned site, relative to the control. At the permafrost boreal forest, T_{20cm} were 3.0–3.4°C higher at the 40 year stand and 4.9–5.4°C higher at the 4 year stand relative to the control. At the nonpermafrost, T_{20cm} were 6.7–7.5°C warmer at the 3 year stand and 2.2–3.2°C warmer at the 15 year old stand (Figure 3d).

Postfire summer soil warming was greater in the boreal forest than in tundra (Figure 4). As a result, postfire summer thaw depths were also deeper in the boreal forest than in the arctic (Figure 4). During snow-covered periods, soil temperatures were lower at the burned sites relative to the unburned control (Figure 4). However, an exception occurred at the 4 year burn in the permafrost boreal forest, where higher upper (0–10 cm) soil temperatures were observed in the winter and spring (Figure 4d).

3.3. Sensitivity Analysis

The effects of postfire organic-layer thickness and soil moisture on soil thermal conductivity in the top 20 cm were partitioned by sensitivity analyses. In tundra, reductions in the organic layer resulted in a 0.16 $W\,m^{-1}\,K^{-1}$ increase in K_{20cm}, while increased soil moisture (i.e., by 20%) resulted in a 0.08 $W\,m^{-1}\,K^{-1}$ increase in K_{20cm} (Figure 5). At the permafrost boreal forest, the organic-layer reduction (i.e., 12 cm loss) resulted in a 0.19 $W\,m^{-1}\,K^{-1}$ increase in K_{20cm}, while increased soil moisture (i.e., by 36%) resulted in a 0.14 $W\,m^{-1}\,K^{-1}$ increase in K_{20cm} (Figure 5). At the nonpermafrost boreal forest, the organic layer reduction resulted in a 0.39 $W\,m^{-1}\,K^{-1}$ increase in K_{20cm}, while increased soil moisture (i.e., by 19%) resulted in a 0.10 $W\,m^{-1}\,K^{-1}$ increase in K_{20cm} (Figure 5).

The effects of postfire organic-layer thickness, surface warming, and soil moisture on soil temperatures in the top 20 cm were partitioned by sensitivity analyses. In tundra, postfire organic layer losses increased T_{20cm} by up to 2.2°C, whereas increased soil moisture caused a 1.1°C increase in T_{20cm}. Surface warming only had a minor effect at the tundra and permafrost boreal forest, causing $<$0.5°C increase in T_{20cm} (Figure 5). Postfire reductions in organic-layer thickness were the most important factor determining soil temperature changes at the nonpermafrost and permafrost boreal forest. Surface warming played the second largest role in soil temperature changes at the nonpermafrost boreal forest (Figure 5).

When perturbations to the organic layer and soil moisture were combined, the impact of the organic layer reduction was more pronounced in moist soil across all tundra and boreal regions. For example, a 12 cm loss in the organic layer caused a 2.6°C increase in T_{20cm} with 30% soil moisture, but a 5.9°C increase in T_{20cm}

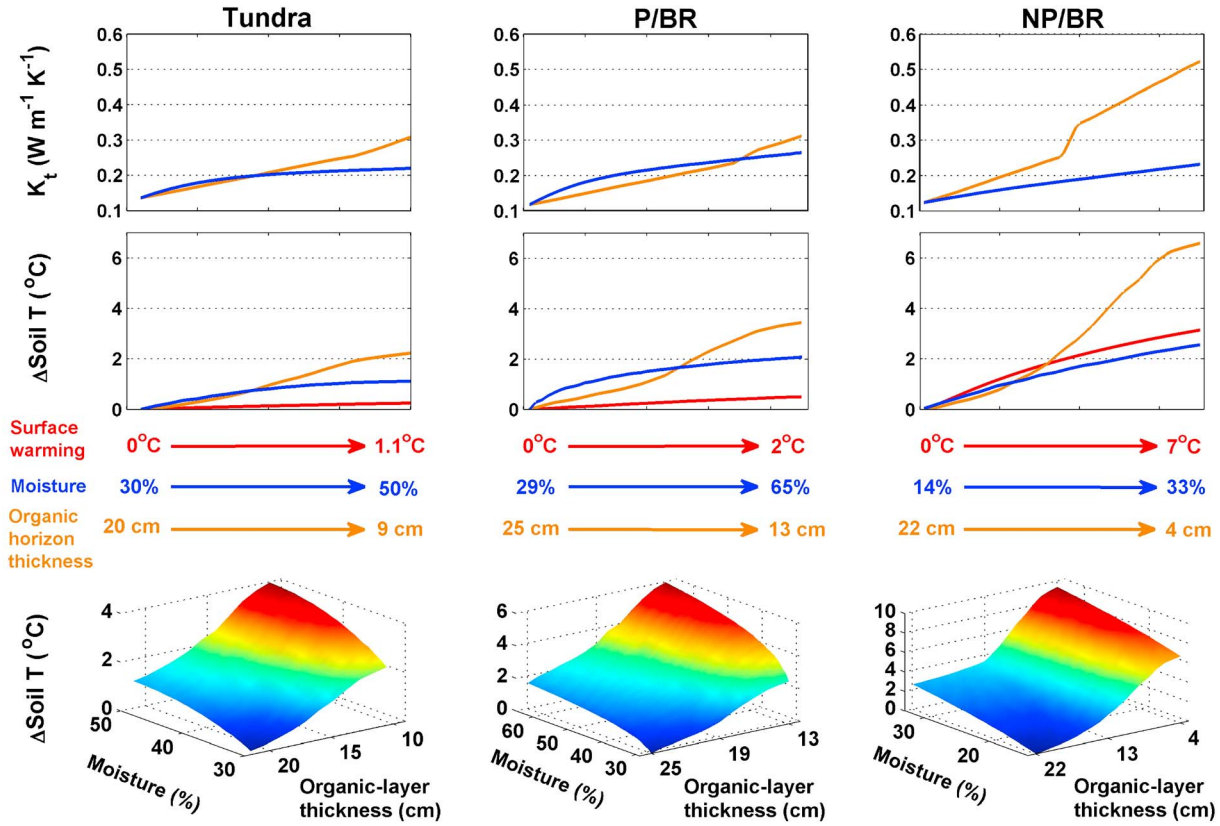

Figure 5. (top) Sensitivity of the mean thermal conductivity in the top 20 cm of soil to soil organic horizon loss and volumetric moisture content change; (middle) sensitivity of soil temperature change at 20 cm to surface warming, soil organic horizon loss, and volumetric moisture content change; (bottom) sensitivity of soil temperature change to the combined perturbations of soil organic horizon loss and volumetric moisture content change over the three studied ecosystems. P represents permafrost, NP represents nonpermafrost, and BR represents boreal forest.

when soil moisture was 65% (Figure 5). Across all sites, increased soil moisture exhibited a positive nonlinear soil temperature change response that saturated at high soil moisture, while soil temperature changes exhibited a nonlinear and nonsaturating positive response to organic-layer thickness.

Comparing soil temperature sensitivities to changes in surface warming, soil moisture, and organic-layer thickness revealed striking differences among ecosystems (Figure 6). In general, tundra was less sensitive to changes in postfire soil properties than the permafrost and nonpermafrost boreal forest. A 1°C surface temperature increase in tundra resulted in a 0.25°C increase in T_{20cm}, but a 0.55°C increase in T_{20cm} in the nonpermafrost boreal forest. A 1% soil moisture increase in tundra resulted in a 0.08°C increase in T_{20cm}, but a 0.15°C increase in T_{20cm} in the nonpermafrost boreal forest. A 1 cm decrease in organic-layer thickness in

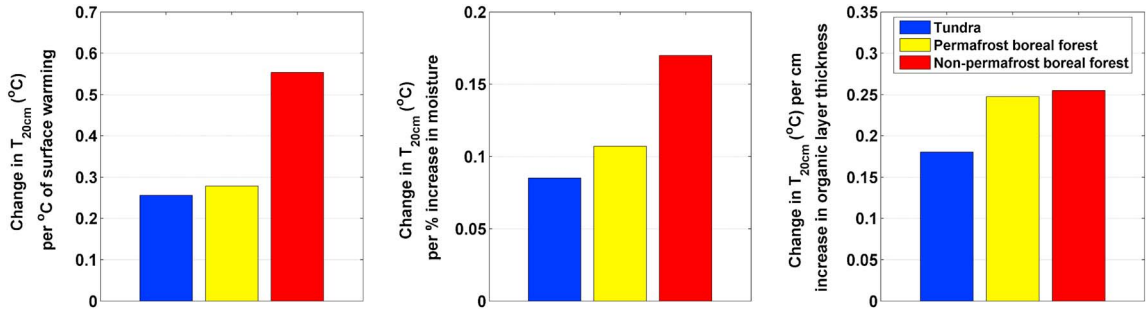

Figure 6. The sensitivity of soil temperatures at the 20 cm soil to per unit change in surface warming (°C), soil moisture (%), and soil organic-layer thickness (cm) in tundra, permafrost boreal forest and nonpermafrost boreal forest.

tundra resulted in a 0.17°C increase in T_{20cm}, but a 0.25°C increase in the nonpermafrost boreal forest. T_{20cm} sensitivities for the permafrost boreal forest fell in between those observed for tundra and the nonpermafrost boreal forest.

3.4. Long-Term Postfire Thaw Depth

Model simulations indicated that the postfire thaw depth increases required decades to recover to unburned levels under all projected warming scenarios. Thaw depth recovery at the severe tundra burn lagged the moderate burn by two decades. At the permafrost boreal forest, both the 4 and 40 year burns required almost a century to recover to unburned levels (Figure 6). A stronger warming scenario generally resulted in a longer thaw depth recovery period.

4. Discussion

In general, the model performed well at each site and closely tracked variations in summer and winter soil temperatures at various depths (Figure 2). In some instances, simulated temperatures deviated from observations, particularly during seasonal transitions in spring and autumn. During these periods, the model underestimated soil temperatures and either froze or thawed soil earlier than was observed (Figure 2). This difference between observed and modeled ground temperature has been reported elsewhere [e.g., *Romanovsky and Osterkamp*, 1997, 2000] and could be attributed to a high latent heat content in permafrost soils or insulation from snow cover that allows soils to stay warmer for a longer period of time. The model was able to simulate summer temperatures reasonably well, and this provided confidence in the comparison of soil thermal states across the different Alaskan ecosystems in summer.

Because we prescribed soil moisture in the top soil layers which included the fire-impact layers, the lack of calibration for hydraulic parameters will not significantly influence the simulations for postfire soil thermal states. For the long-term simulations, the direct effect of moss recovery on hydraulic conductivity was not considered. However, the moss changes may not have strong effect on the water cycle at tundra sites, where the near-surface soils were always highly saturated [*Giblin et al*., 1991]. In permafrost boreal forest, the increase in soil moisture at burned stand may be partly due to the fire-caused change in hydraulic conductivities of the near-surface soil. Therefore, the parameters we used for hydraulic conductivities may underestimate the soil moisture at the top layer. Based on our sensitivity analysis (Figure 5), it may cause at most 2°C underestimation of T_{20cm} assuming the fire-caused increase in soil moisture was completely due to changes in hydraulic conductivity. However, as the moss and organic layer recovered, the impact of the underestimation of soil moisture on soil thermal state became smaller and it will not significantly influence the timing of the recovery of thaw depth.

Our study utilized a permafrost and ecosystem gradient to develop a mechanistic understanding of the short- and long-term impacts of tundra and boreal forest fires on soil thermal dynamics. Data and modeling indicated that (1) fires affect soil temperature and thaw depth for decades (Figures 3 and 7), (2) soil moisture interacts with the surface energy budget and soil thermal regime to both positively and negatively impact soil and surface temperature (Figures 3, 5, and 6), and (3) permafrost played a large role in buffering postfire soil and surface temperature increases (Figures 3, 4, and 6).

4.1. How Did Fire Influence Soil Temperature and Thaw Depth?

Fire increased both soil temperature and thaw depth across tundra and boreal forest ecosystems (Figures 3 and 4). These increases were largely attributed to soil organic layer combustion losses that increased soil thermal conductivity for decades after fire (Figures 5 and 7). The organic layer is less conductive than the underlying mineral layer, and its loss increased the efficiency of heat transfer throughout the soil column, resulting in warmer and deeper soils after fire [*Yoshikawa et al*., 2003; *O'Donnell et al*., 2009]. The importance of the organic layer in determining postfire soil temperatures, and thaw depth indicates that greater attention should be paid on its loss through increased burn severity. Comparison across the three ecosystems indicates that burn severity was greatest in the nonpermafrost boreal forest and lowest in the tundra. These burn severity differences likely arose from the presence of higher water tables at the permafrost sites and differences in flammability between boreal and tundra ecosystems. A greater loss of the organic layer has consequences for postfire recovery of soil temperature and thaw depth in these systems. For example,

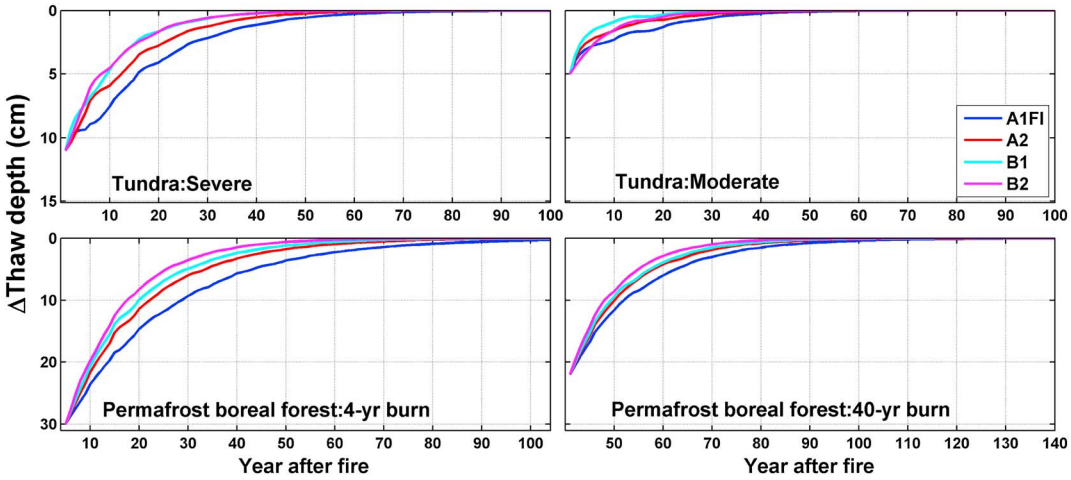

Figure 7. The difference in simulated thaw depth (cm) between burned and unburned site in the tundra and the permafrost boreal forest after the fire year under four projected future climate scenarios, with considering the recovery of moss, fibrous, and amorphous organic horizons.

both the boreal forest and the severely burned tundra will require several decades longer than moderately burned tundra to remove the fire effect on soil temperature and thaw depth because of the deeper burning of the soil organic layer (Figure 7).

4.2. What Other Factors Influenced Soil Temperature and Thaw Depth?

Soil temperature and thaw depth were also influenced by soil moisture, changes to the surface energy budget, and the presence of permafrost. In many cases, interactions among these three factors made attribution of their effect on soil temperatures and thaw depth difficult. However, the combination of modeling and in situ measurements across the three ecosystem types allowed us to assess their relative impact on postfire soil temperature and thaw depth changes. In general, increased soil moisture and surface temperature increased soil temperatures with soil moisture changes having a larger role than surface temperature. Increased soil moisture directly impacted soil temperature by increasing soil thermal conductivity, while surface temperature indirectly impacted soil temperatures by altering energy availability to warm the soil. These changes to energy availability were largely realized by postfire alterations to energy partitioning as evidenced by warmer postfire soil temperatures that persisted beyond the recovery of albedo (Figure 3).

Postfire soil moisture changes were inconsistent across ecosystems with some experiencing large changes in soil moisture and others little change (Table 1). Average postfire soil moisture did not vary in tundra, even though greater surface water pooling was observed at the burned sites [*Rocha and Shaver*, 2011; A. V. Rocha, personal observation, 2012]. The inability of soil moisture measurements to capture these dynamics may be attributed to measurement limitations in characterizing the heterogeneous landscape. At the permafrost boreal forest, postfire increases in soil moisture were observed at both the 3 and 40 year old stand. These increases likely resulted from reduced rates of transpiration from decreased canopy leaf area, poor surface drainage from the presence of permafrost, and energy budget changes at the top of the soil [*Moody and Martin*, 2001]. At the nonpermafrost boreal forest, postfire soil moisture slightly decreased at the young stands likely because of the loss of the water-absorbing organic layer and the deep soils which allowed for greater drainage.

Soil moisture also influenced the energy balance with large impacts on surface temperatures. Summer surface temperatures greatly increased after fire at the nonpermafrost boreal forest, but only slightly increased or decreased in tundra and permafrost boreal forest. At the tundra fire scar, surface temperature differences were mostly attributed to changes in energy partitioning (Table 1). At the burned tundra sites, latent heat flux increased ~14.0–15.6 W/m^2, *Rocha and Shaver* [2011] after fire from the evaporation of surface water pools. This effect limited surface warming and resulted in similar surface temperature across the burn severity gradient. In the boreal forest, the presence of permafrost impacted surface temperatures

with the effect of cooling the surface. Permafrost cooled the surface by creating a large heat sink, impeding drainage, increasing surface water pooling [*Harden et al*., 2006; *Osterkamp and Burn*, 2002; *Jorgenson and Osterkamp*, 2005] (Figure 3b). Like tundra, greater postfire surface water pooling increased evapotranspiration and cooled the surface in the permafrost boreal forest. The lack of permafrost at the nonpermafrost boreal forest resulted in the highest postfire surface temperature changes observed across the three ecosystems (Figure 3).

4.3. What Are the Implications of Our Findings?

The difference between summer (unfrozen) and winter (frozen) thermal conductivity gives rise to the "thermal offset" (the difference in mean annual temperatures at the permafrost table and at the ground surface [*Burn and Smith*, 1988; *Romanovsky and Osterkamp*, 1997]). Thermal offset is generated by the difference in frozen and unfrozen thermal conductivities at a site. Compared with dry sites, wet sites tend to have higher thermal offsets because the difference in thermal conductivity in summer and winter is larger [*Burn and Smith*, 1988; *Osterkamp and Burn*, 2002]. Thermal offset has great implications on the ground thermal regime in permafrost areas. For example, it allows for annual mean ground surface temperatures warmer than 0°C to exist over multiyear periods while still preserving permafrost [*Osterkamp and Burn*, 2002]. At the burned site, the increased active layer thickness can lead to larger thermal offset [*Romanovsky and Osterkamp*, 1997]. Meanwhile, the postfire changes in soil moisture also have important effect on thermal offset. In this study, the postfire wetting in upland stands (e.g., the burned Hess Creek sites) may reduce rates of further thaw, because of the increased thermal offset. As a consequence, less C will transfer from a frozen to thawed state, and thus lower decomposition. Moreover, the saturation and anoxic conditions caused by postfire wetting can also reduce postthaw C loss from the soil. In contrast, a possible postfire drying (lower thermal offset) condition can increase the vulnerability of permafrost to future thaw and increase the C loss from the soil. This mechanism emphasizes that the postfire changes in thermal offset reflect local changes in soil thermal properties that can facilitate recovery or further degradation of permafrost following disturbance.

Our results highlight important differences in postfire soil temperatures and thaw depths among tundra, and permafrost and nonpermafrost boreal forests. These differences have important implications for the vulnerability of permafrost and feedbacks to future climate change. Permafrost is especially vulnerable following fires because of the long-term warming impacts that are dependent upon the thickness of the soil organic layer and its ability to reform. Results from the climate and ecosystem gradient utilized here indicates that soil temperatures will be more sensitive to postfire changes in soil properties under a warmer climate (Figure 6). Warmer ecosystems without permafrost tend to lose more of their organic layer and alter their energy balance to increase soil temperatures more than ecosystems with permafrost. Ecosystems in colder climates also more buffered against postfire soil temperature increases because permafrost formation in these regions are dictated by climate rather than ecosystem factors [*Shur and Jorgenson*, 2007]. Consequently, tundra permafrost is also less sensitive to postfire soil changes than in the boreal forest because its reformation is driven more by the continuing cold air temperatures than by moss and the organic-layer thickness recovery. However, in some parts of the boreal forest, permafrost is largely maintained by ecosystem factors such as the insulating organic layer. In these areas, postfire decreases to the organic layer can result in irreversible loss of the underlying permafrost. As climate warms, permafrost in these areas will be increasingly sensitive to postfire changes to soil properties, highlighting the importance of understanding interactions among climate, organic-layer thickness losses, and its recovery.

Acknowledgments

We thank Heping Liu and James T. Randerson for providing the soil temperature and moisture data sets for the three studied Delta Junction sites and thank Kemal Gökkaya for comments on earlier drafts of this manuscript. We are pleased to acknowledge funding from the US National Science Foundation, grants DEB-1026843 and EF-1065587, to the Marine Biological Laboratory. Additional logistical support was provided by Toolik Field Station and CH2MHill, funded by NSF's Office of Polar Programs.

References

Balshi, M. S., A. D. McGuire, P. Duffy, M. Flannigan, D. W. Kicklighter, and J. Melillo (2009), Vulnerability of carbon storage in North American boreal forests to wildfires during the 21st century, *Global Change Biol.*, *15*, 1491–1510.

Bret-Harte, M. S., M. C. Mack, G. R. Shaver, D. C. Huebner, M. Johnston, C. A. Mojica, M. C. Pizano, and J. A. Reiskind (2013), The response of Arctic vegetation and soils following an unusually severe tundra fire, *Philos. Trans. R. Soc. B*, *368*(1624), 20120490, doi:10.1098/rstb.2012.0490.

Burn, C., and C. Smith (1988), Observations of the "thermal offset" in near-surface mean annual ground temperatures at several sites near Mayo, Yukon Territory, Canada, *Arctic*, *41*(2), 99–104.

Chambers, S. D., and F. S. Chapin III (2002), Fire effects on surface-atmosphere energy exchange in Alaskan black spruce ecosystems: Implications for feedbacks to regional climate, *J. Geophys. Res.*, *107*(D1), 8145, doi:10.1029/2001JD000530.

Chambers, S. D., J. Beringer, J. T. Randerson, and F. S. Chapin III (2005), Fire effects on net radiation and energy partitioning: Contrasting responses of tundra and boreal forest ecosystems, *J. Geophys. Res.*, *110*, D09106, doi:10.1029/2004JD005299.

Fayer, M. J. (2000), UNSAT-H Version 3.0: Unsaturated soil water and heat flow model: Theory, user manual, and examples, Report, Pac. Northwest Natl. Lab., Richland, Wash.
Giblin, A. E., K. J. Nadelhoffer, G. R. Shaver, J. A. Laundre, and A. J. McKerrow (1991), Biogeochemical diversity along a riverside toposequence in Arctic Alaska, *Ecol. Monogr.*, *61*, 415–435.
Hansson, K., J. Šimůnek, M. Mizoguchi, L. Lundin, and M. T. van Genuchten (2004), Water flow and heat transport in frozen soil: Numerical solution and freeze–thaw applications, *Vadose Zone J.*, *3*, 693–704.
Harden, J. W., K. P. O'Neill, S. E. Trumbore, H. Veldhuis, and B. J. Stocks (1997), Moss and soil contributions to the annual net carbon flux of a maturing boreal forest, *J. Geophys. Res.*, *102*, 28,805–28,816, doi:10.1029/97JD02237.
Harden, J. W., K. L. Manies, M. R. Turetsky, and J. C. Neff (2006), Effects of wildfire and permafrost on soil organic matter and soil climate in interior Alaska, *Global Change Biol.*, *12*, 2391–2403.
Harden, J. W., K. L. Manies, J. O'Donnell, K. Johnson, S. Frolking, and Z. Fan (2012), Spatiotemporal analysis of black spruce forest soils and implications for the fate of C, *J. Geophys. Res.*, *117*, G01012, doi:10.1029/2011JG001826.
Hinkel, K. M., and F. E. Nelson (2003), Spatial and temporal patterns of active layer thickness at Circumpolar Active Layer Monitoring (CALM) sites in northern Alaska, 1995–2000, *J. Geophys. Res.*, *108*(D2), 8168, doi:10.1029/2001JD000927.
Hu, F. S., P. E. Higuera, J. E. Walsh, W. L. Chapman, P. A. Duffy, L. B. Brubaker, and M. L. Chipman (2010), Tundra burning in Alaska: Linkages to climatic change and sea ice retreat, *J. Geophys. Res.*, *115*, G04002, doi:10.1029/2009JG001270.
Iman, R. L., and J. C. Helton (1988), An investigation of uncertainty and sensitivity analysis techniques for computer models, *Risk Anal.*, *8*, 71–90, doi:10.1111/j.1539-6924.1988.tb01155.x.
Intergovernmental Panel on Climate Change (2007), *Contribution of Working Group III to the Fourth Assessment Report of the Intergovernmental Panel on Climate Change*, edited by B. Metz et al., Cambridge Univ. Press, Cambridge, U. K., and New York.
Jafarov, E. E., V. E. Romanovsky, H. Genet, A. D. McGuire, and S. S. Marchenko (2013), The effects of fire on the thermal stability of permafrost in lowland and upland black spruce forests of interior Alaska in a changing climate, *Environ. Res. Lett.*, *8*, 035030.
Jiang, Y., Q. Zhuang, and J. A. O'Donnell (2012), Modeling thermal dynamics of active layer soils and near-surface permafrost using a fully coupled water and heat transport model, *J. Geophys. Res.*, *117*, D11110, doi:10.1029/2012JD017512.
Johnstone, J. F., F. S. Chapin III, T. N. Hollingsworth, M. C. Mack, V. Romanovsky, and M. Turetsky (2010), Fire, climate change, and forest resilience in interior Alaska, *Can. J. For. Res.*, *40*, 1302–1312.
Jorgenson, M. T., and T. E. Osterkamp (2005), Response of boreal ecosystems to varying modes of permafrost degradation, *Can. J. For. Res.*, *35*, 2100–2111.
Kasischke, E. S., and J. F. Johnstone (2005), Variation in postfire organic layer thickness in a black spruce forest complex in interior Alaska and its effects on soil temperature and moisture, *Can. J. For. Res.*, *35*(9), 2164–2177.
Kasischke, E. S., and M. R. Turetsky (2006), Recent changes in the fire regime across the North American boreal region—Spatial and temporal patterns of burning across Canada and Alaska, *Geophys. Res. Lett.*, *33*, L09703, doi:10.1029/2006GL025677.
Kasischke, E. S., et al. (2010), Alaska's changing fire regime-implications for the vulnerability of its boreal forests, *Can. J. For. Res.*, *40*, 1313–1324.
Liljedahl, A., L. Hinzman, R. Busey, and K. Yoshikawa (2007), Physical short-term changes after a tussock tundra fire, Seward Peninsula, Alaska, *J. Geophys. Res.*, *112*, F02S07, doi:10.1029/2006JF000554.
Liu, H., and J. T. Randerson (2008), Interannual variability of surface energy exchange depends on stand age in a boreal forest fire chronosequence, *J. Geophys. Res.*, *113*, G01006, doi:10.1029/2007JG000483.
Liu, H., J. T. Randerson, J. Lindfors, and F. S. Chapin III (2005), Changes in the surface energy budget after fire in boreal ecosystems of interior Alaska: An annual perspective, *J. Geophys. Res.*, *110*, D13101, doi:10.1029/2004JD005158.
Manies, K. L., J. W. Harden, S. R. Silva, P. H. Briggs, and B. M. Schmid (2004), Soil data from *Picea mariana* stands near Delta Junction, Alaska of different ages and soil drainage type, *U.S. Geol. Surv. Open File Rep., 2004–1271*.
Moody, J. A., and D. A. Martin (2001), Post-fire rainfall intensity-peak discharge relations for three mountainous watersheds in the western USA, *Hydrol. Processes*, *15*, 2981–2993.
Noborio, K., K. J. McInnes, and J. L. Heilman (1996), Two-dimensional model for water, heat and solute transport in furrow-irrigated soil: I. Theory, *Soil Sci. Soc. Am. J.*, *60*, 1001–1009.
O'Donnell, J. A., V. E. Romanovsky, J. W. Harden, and A. D. McGuire (2009), The effect of soil moisture content on the thermal conductivity of soil organic horizons in black spruce ecosystems of interior Alaska, *Soil Sci.*, *174*, 646–651.
O'Donnell, J. A., J. W. Harden, A. D. McGuire, and V. E. Romanovsky (2011a), Exploring the sensitivity of soil carbon dynamics to climate change, fire disturbance and permafrost thaw in a black spruce ecosystem, *Biogeosciences*, *8*, 1367–1382.
O'Donnell, J. A., J. W. Harden, A. D. McGuire, M. Z. Kanevskiy, M. T. Jorgenson, and X. Xu (2011b), The effect of fire and permafrost interactions on soil carbon accumulation in an upland black spruce ecosystem of interior Alaska: Implications for post-thaw carbon loss, *Global Change Biol.*, *17*, 1461–1474.
Osterkamp, T. E., and C. R. Burn (2002), Permafrost, in *Encyclopedia of Atmospheric Sciences*, edited by J. R. Holton, J. Pyle, and J. A. Curry, pp. 1717–1729, Academic Press, San Diego, Calif.
Rocha, A. V., and G. R. Shaver (2009), Advantages of a two band EVI calculated from solar and photosynthetically active radiation fluxes, *Agric. For. Meteorol.*, *149*, 1560–1563, doi:10.1016/j.agrformet.2009.03.016.
Rocha, A. V., and G. R. Shaver (2011), Postfire energy exchange in arctic tundra: The importance and climatic implications of burn severity, *Global Change Biol.*, *17*, 2831–2841.
Rocha, A. V., M. M. Loranty, P. E. Higuera, M. C. Mack, F. S. Hu, B. M. Jones, A. L. Breen, E. B. Rastetter, S. J. Goetz, and G. R. Shaver (2012), The footprint of Alaskan tundra fires during the past half-century: Implications for surface properties and radiative forcing, *Environ. Res. Lett.*, *7*, 044039, doi:10.1088/1748-9326/7/4/044039.
Romanovsky, V. E., and T. E. Osterkamp (1997), Thawing of the active layer on the coastal plain of the Alaskan Arctic, *Permafrost Periglacial Processes*, *8*, 1–22.
Romanovsky, V. E., and T. E. Osterkamp (2000), Effects of unfrozen water on heat and mass transport processes in the active layer and permafrost, *Permafrost Periglacial Processes*, *11*, 219–239.
Saito, H., J. Šimůnek, and B. P. Mohanty (2006), Numerical analysis of coupled water, vapor, and heat transport in the vadose zone, *Vadose Zone J.*, *5*, 784–800.
Schuur, E. A. G., et al. (2008), Vulnerability of permafrost carbon to climate change: Implications for the global carbon cycle, *BioScience*, *58*, 701–714.
Shur, Y. L., and M. T. Jorgenson (2007), Patterns of permafrost formation and degradation in relation to climate and ecosystems, *Permafrost Periglacial Processes*, *18*, 7–19, doi:10.1002/ppp.582.

Welp, L. R., J. T. Randerson, and H. P. Liu (2007), The sensitivity of carbon fluxes to spring warming and summer drought depends on plant functional type in boreal forest ecosystems, *Agric. For. Meteorol.*, *147*, 172–185.

Yi, S., et al. (2009a), Interactions between soil thermal and hydrological dynamics in the response of Alaska ecosystems to fire disturbance, *J. Geophys. Res.*, *114*, G02015, doi:10.1029/2008JG000841.

Yi, S., K. Manies, J. Harden, and A. D. McGuire (2009b), Characteristics of organic soil in black spruce forests: Implications for the application of land surface and ecosystem models in cold regions, *Geophys. Res. Lett.*, *36*, L05501, doi:10.1029/2008GL037014.

Yi, S., A. D. McGuire, E. S. Kasischke, J. Harden, K. Manies, M. Mack, and M. Turetsky (2010), A dynamic organic soil biogeochemical model for simulating the effects of wildfire on soil environmental conditions and carbon dynamics of black spruce forests, *J. Geophys. Res.*, *115*, G04015, doi:10.1029/2010JG001302.

Yoshikawa, K., W. R. Bolton, V. E. Romanovsky, M. Fukuda, and L. D. Hinzman (2003), Impacts of wildfire on the permafrost in the boreal forests of Interior Alaska, *J. Geophys. Res.*, *108*(D1), 8148, doi:10.1029/2001JD000438.

Yuan, F. M., S. H. Yi, A. D. McGuire, K. D. Johnson, J. J. Liang, J. W. Harden, E. Kasischke, and W. A. Kurz (2012), Assessment of historical boreal forest carbon dynamics in the Yukon river basin: Relative roles of climate warming and fire regime changes, *Ecol. Appl.*, *22*, 2091–2109.